

# Relationship Between the Initiation and Propagation of SCC and the Electrochemical Noise of Alloy 600 for the Steam Generator Tubing of Nuclear Power Plants

Y. S. Kim<sup>1,†</sup>, H. S. Nam<sup>2</sup>, Y. H. Kwon<sup>1</sup>, S. W. Kim<sup>3</sup>, H. P. Kim<sup>3</sup>, and H. Y. Chang<sup>4</sup>

<sup>1</sup>The Center for Green Materials Technology, School of Advanced Materials Engineering, Andong National University, 388 Songcheon-dong, Andong, Gyeongbuk 760-749, Korea

<sup>2</sup>HanShin S-Meca, 509 Wanpyeon-Dong, Yuseong, Daejeon 350-509, Korea

<sup>3</sup>Korea Atomic Energy Research Institute, P. O. Box 105, Yuseong, Daejeon 305-600 Korea

<sup>4</sup>Korea Power Engineering Company, 257 Yonggudaero, Yongin, Gyeonggi, 446-912, Korea

(Received February 10, 2010; Revised March 22 2010; Accepted March 31, 2010)

Since nuclear power plants are being operated under high temperature and high pressure, on-line monitoring technique to detect corrosion could be more effective than off-line method in shut-off period. In this operating condition, electrochemical noise method may be suitable to monitor the corrosion. This paper aims the analysis on the relation between the cracking and electrochemical noise signal of Alloy 600 under U-bending. When electrochemical noise monitoring technique was used during SCC test, it was judge to be obvious that if cracks generate, its generation can be detected by electrochemical current noise. Cracking-related noise was defined as the noise showing 5~10 times greater than the average value of background noise bands. On the base of crack noise, crack initiation time was determined. From SCC test and electrochemical noise monitoring in 25 °C, 0.1 M Na<sub>2</sub>S<sub>4</sub>O<sub>6</sub> solution (Reverse U-Bended Alloy 600 SE+), average crack initiation time was obtained as 9,046 seconds and from its initiation time, it could be defined that net crack propagation rate is the crack length divided by  $\Delta T$ (= total test period - crack initiation time). Therefore, average net crack propagation rate was obtained to be  $1.18 \times 10^{-9}$  m/s.

**Keywords** : alloy 600, stress-corrosion cracking, crack initiation time, crack propagation rate, electrochemical noise

## 1. Introduction

Since Kori unit 1 nuclear power plant has begun commercially to operate in 1978, 20 units in Uljin, Wolsong, and Yeonggwang are currently being operated and the are sharing 40% of domestic electric power.<sup>1)</sup>

In pressurized water reactor, the reactor and pressurizer yield the primary water in high temperature and high pressure which steam is generated in the steam generator (S/G) by heat transfer from the primary water to the secondary water. Steam operates the turbine generating the electric power. Many problems including wastage, denting, pitting, fretting, SCC (Stress Corrosion Cracking), intergranular attack have occurred in nuclear power plants because of high pressure, load, and temperature. Among these problems, SCC is a main corrosion damage. SCC is characterized to have brittle fracture as materials are subjected

to tensile stress in specific corrosion environment. The occurrence of SCC may be extended to radiation accidents, shut-down and economic loss from increased maintenance cost.<sup>2)-8)</sup>

Steam generators of pressurized water reactors have used Alloy 600 and Alloy 690 as the tubing. Alloy 600 and Alloy 690 meets the requirement of design and have shown good corrosion resistance. However, since the facilities have been operated in continuous and long periods, S/G tubing has been suffered from SCC and repaired by means of sleeving and plugging. Some of steam generators have experiences to be replaced by new ones in extreme cases.<sup>9)</sup> Therefore, new technologies are needed to be applied for monitoring and controlling corrosion damages including SCC in nuclear power plants.

Corrosion monitoring techniques can be categorized as weight loss method, electrochemical method, surface activation method and ultrasonic method. Electrochemical monitoring methods include polarization, current monitor-

<sup>†</sup> Corresponding author: [yikim@andong.ac.kr](mailto:yikim@andong.ac.kr)

ing, linear polarization, electrochemical impedance, electrochemical potential noise measurement, electrochemical current noise measurement, and zero resistance ammeter techniques.

Since nuclear power plants are operating under high temperature and high pressure, on-line monitoring technique in operating plants could be more effective than off-line method in shut-off period. In this condition, electrochemical noise method can be suitable to monitor the corrosion. Electrochemical noise methods was developed by Iverson in 1968<sup>10</sup> and it could give useful information about electrochemical reaction.<sup>11)-12)</sup> Furthermore, during last 10 years, electrochemical technique has shown the beneficial effect on the energy-related industry including oil and gas plants and nuclear power plants that are exposed to aggressive corrosive environments. Researchers are trying to improve further the accuracy and applicability of electrochemical noise method until now.<sup>11),13)-20)</sup>

Corrosion monitoring method using electrochemical noise method is applied to the field of pitting and stress corrosion cracking. Electrochemical noise monitoring on pitting corrosion are performed on 409 stainless steels in 0.6 M NaCl+0.1M HCl.<sup>13)</sup> The effect of nonmetallic inclusions on the localized corrosion of 2507 duplex stainless steel in 80 °C 4 M NaCl was investigated.<sup>10)</sup>

Stress corrosion cracking tests include constant load test, slow strain rate test(SSRT) and constant strain tests(C-ring, U-bending). Using the electrochemical noise method, the relation was investigated between measured noise and cracking of 304 stainless steel under U-bend and slow rate load in magnesium chloride solution.<sup>21)</sup> It was found that typical characteristics of the electrochemical noise fluctuations generated by SCC were varied with corrosion system. Sulfur has been identified as one of the major impurities introduced into the secondary water of pressurized water reactors.<sup>22)</sup> Under steam generator operating conditions, sulfates are reduced by hydrazine to lower-valence sulfur species, such as tetrathionate, thiosulfate, or sulfide. Many researchers have investigated the effect of sulfur-species on the SCC of Alloy 600,<sup>22)-25)</sup> but they didn't try to use the electrochemical noise technique to detect the initiation of SCC.

As reviewed above, many studies on pitting and SCC by electrochemical noise method have been reported but there are few about relations between cracking and electrochemical noise signal. Therefore, the purpose of this paper is to analyze the relation between cracking and electrochemical noise signal of Alloy 600 under U-bending.

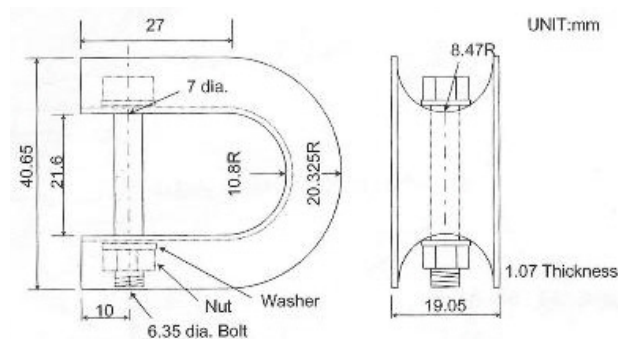


Fig. 1. Dimension of RUB specimen.

## 2. Experimental procedures

### 2.1 Materials

#### 2.1.1 Heat treatment

Alloy 600 tubing(diameter : 19.05 mm) was solution annealed at 1100 °C for 30 minutes (Alloy 600MA(Mill Annealed), Ni-17.3Cr-10.1Fe-0.03C). Alloy 600SE+ was sensitized at 600 °C for 48 hours.

#### 2.1.2 RUB(Reverse U-bend) specimen

Alloy 600 tubing was bisected longitudinally by wire-cutting method and then the holes were created with drilling for bolt-tightening after U-Bending. The bi-sectioned tubing was reverse U-bended by the mandrill. The inside of tubing was ground gradually up to #2000 using SiC paper and cleaned with acetone, methyl alcohol and distilled water using an ultrasonic cleaner. Fig. 1 shows the dimension of RUB specimen.

### 2.2 SCC test and electrochemical noise monitoring

SCC test was performed in deaerated 25 °C, 0.1 M Na<sub>2</sub>S<sub>4</sub>O<sub>6</sub> and saturated calomel electrode was used as a reference electrode. The unstrained Alloy 600 bi-sectioned tubing was used as counter electrode. During the test, electrochemical noise was measured using EN 120 program(Gamry co.) under open circuit potential at 1 Hz. After SCC test, liquid penetration test(GS Chem. Ltd) was applied and the cracked areas (surface and cross section) were observed with OM(Axiotech 100HD, Zeiss) and SEM(JEOL, JSM-6300).

### 2.3 Microstructure observation

Microstructure and carbide precipitation were respectively observed by etching in HCl 80 ml + HNO<sub>3</sub> 20 ml and H<sub>3</sub>PO<sub>4</sub> 80 ml + distilled water 10 ml at room temperature.

### 3. Results and discussion

In order to find the relationship between electrochemical noise and SCC initiation, Alloy 600 SE+ was tested in 0.1 M Na<sub>2</sub>S<sub>4</sub>O<sub>6</sub> at 25 °C. Na<sub>2</sub>S<sub>4</sub>O<sub>6</sub> solution facilitates the formation of stress corrosion cracking - sulfur ions adsorb on the oxide surface and form voids. Then the oxide layer

becomes unstable and finally cracked.

Fig. 2 shows (a) electrochemical current noise and (b) electrochemical potential noise measured during SCC test in 25 °C, 0.1 M Na<sub>2</sub>S<sub>4</sub>O<sub>6</sub> solution. Reverse U-Bended Alloy 600 SE+ was used and electrochemical noise was measured for 132 hours in 1 Hz using EN120(Gamry co.). In general, if corrosion takes place, electrochemical current

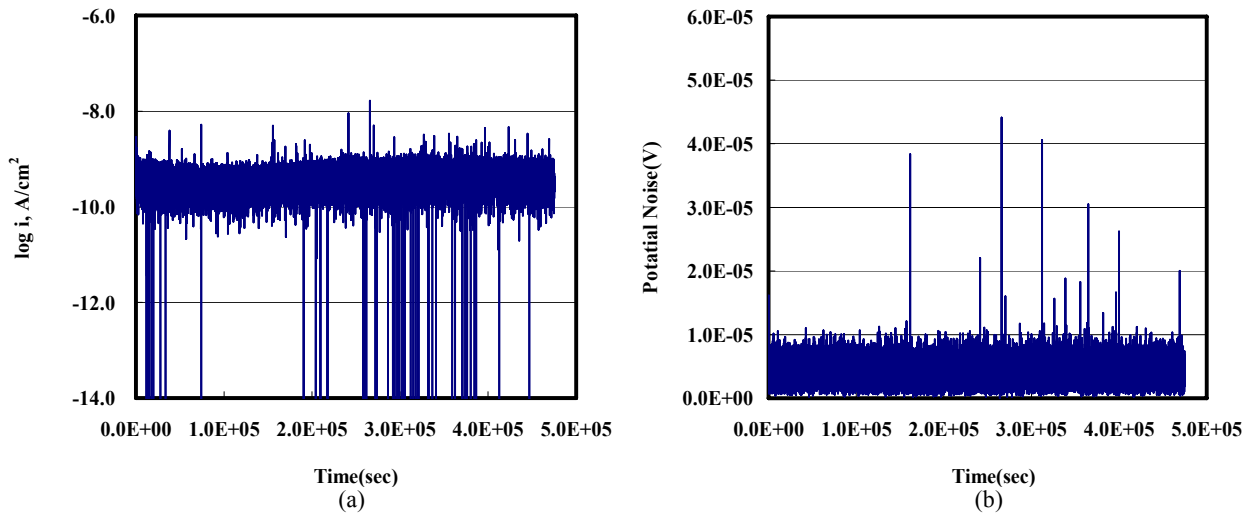


**Fig. 2.** (a) Current Noise and (b) Potential Noise measured during stress corrosion cracking test in 25 °C, 0.1 M Na<sub>2</sub>S<sub>4</sub>O<sub>6</sub> solution (Reverse U-Bended Alloy 600 SE+, Noise was measured for 132 hours in 1 Hz).

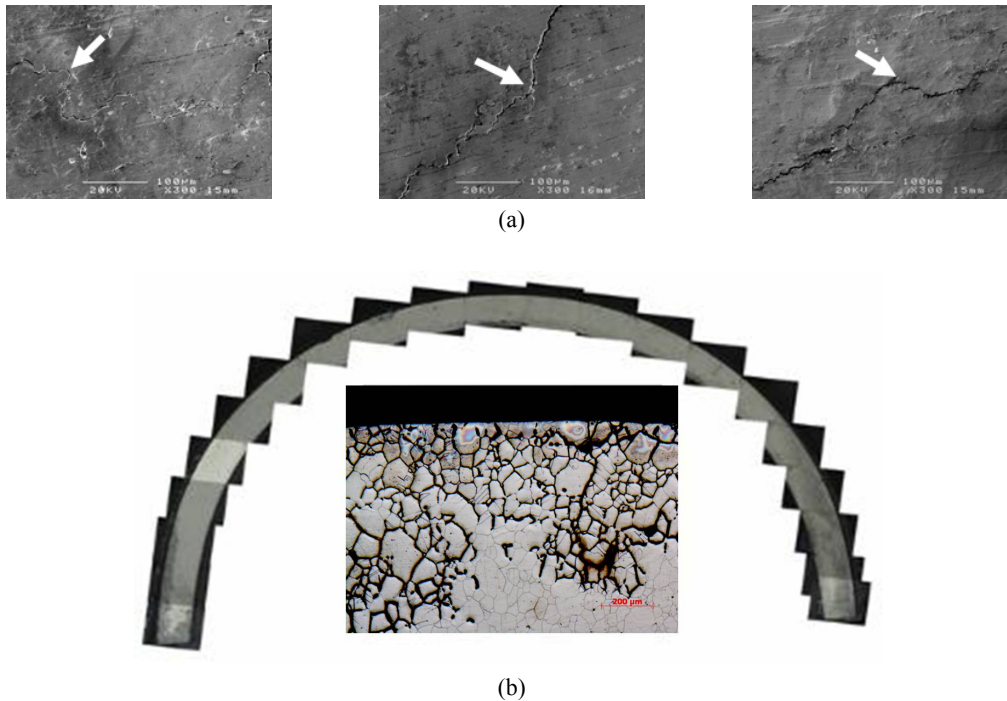


**Fig. 3.** Surface and cross section morphology after SCC test (reverse U-bending specimen) for 132 hrs of Alloy 600 SE+ in 25 °C 0.1 M Na<sub>2</sub>S<sub>4</sub>O<sub>6</sub> solution.

noise will show positive value and potential noise will show negative value than those of background noise.<sup>10)</sup> As shown in Fig. 1, many negative noise peaks were generated in case of current noise and lots of positive potential noise peaks were formed in case of potential noise. Therefore, negative current noise peaks and positive potential noise peaks are meaningless and thus those should

be discarded. As shown in Fig. 2(a), background current noise bands having a range of  $10^{-9}\sim 10^{-10}$  A/cm<sup>2</sup> were obtained. 92 cracking-related noises that were higher than noise bands were detected and first noise started at 1,110 seconds after testing. As shown in Fig. 2(b), background potential noise bands under  $1\cdot 10^{-5}$  V were obtained but almost positive potential noise bands were detected.

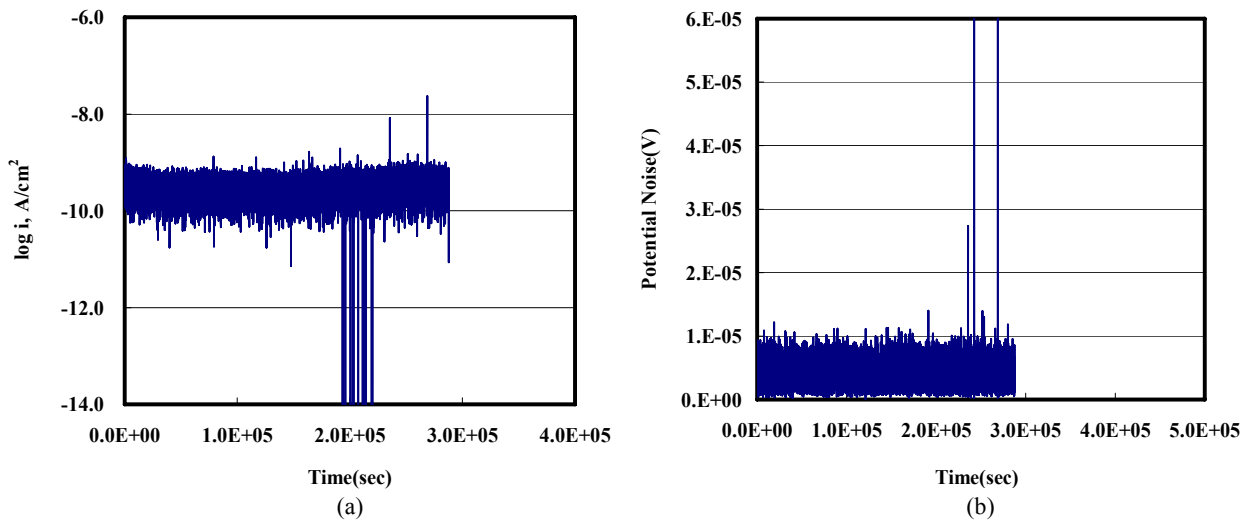


**Fig. 4.** (a) Current Noise and (b) Potential Noise measured during stress corrosion cracking test in 25 °C, 0.1 M Na<sub>2</sub>S<sub>4</sub>O<sub>6</sub> solution (Reverse U-Bended Alloy 600 SE+, Noise was measured for 80 hours in 1 Hz).

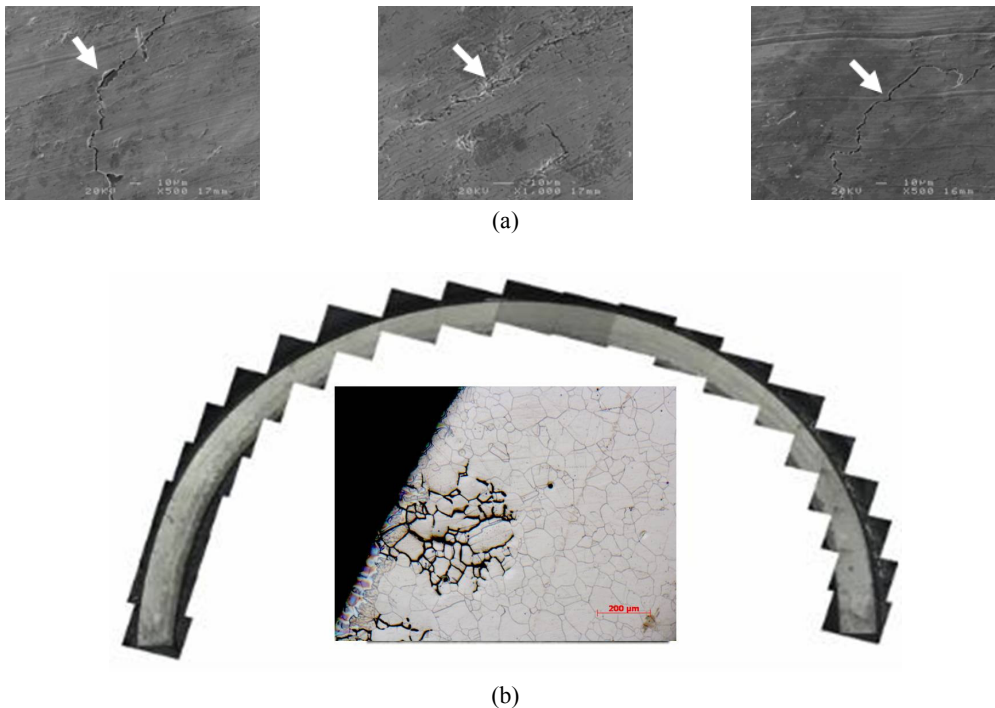


**Fig. 5.** Surface and cross section morphology after SCC test (reverse U-bending specimen) for 80 hrs of Alloy 600 SE+ in 25 °C 0.1 M Na<sub>2</sub>S<sub>4</sub>O<sub>6</sub> solution.

Therefore, it seems reasonable to judge that electrochemical current noise rather than electrochemical potential noise is more sensitive to detect SCC.

Fig. 3 shows surface and cross section morphology after SCC test (reverse U-bending specimen) for 132 hours of Alloy 600 SE+ in 25 °C 0.1 M Na<sub>2</sub>S<sub>4</sub>O<sub>6</sub> solution. The specimen was cleaned after SCC test and in order to confirm the generation of crack, penetration test was performed. Fig. 3(a) shows SEM images of apex area and many cracks were observed. Fig. 3(b) shows the cross sectional images by optical microscope of reverse U-bending tube. Cracking mode was confirmed as intergranular cracking and most of cracks were generated near apex ± 30°.

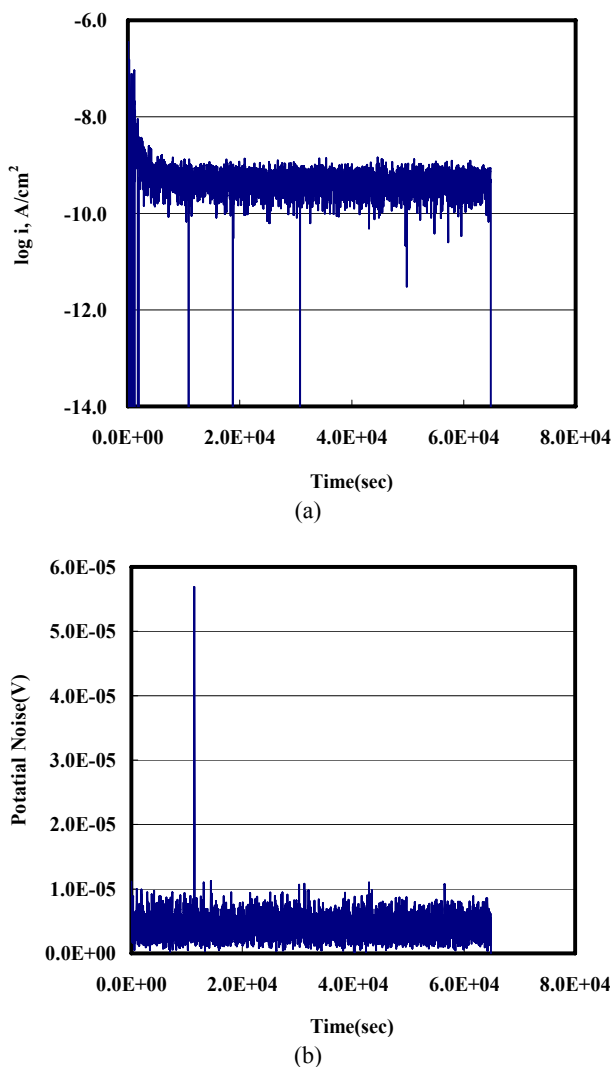


**Fig. 6.** (a) Current Noise and (b) Potential Noise measured during stress corrosion cracking test in 25 °C, 0.1 M Na<sub>2</sub>S<sub>4</sub>O<sub>6</sub> solution (Reverse U-Bended Alloy 600 SE+, Noise was measured for 18 hours in 1 Hz).

Fig. 4 shows (a) current noise and (b) potential noise measured during stress corrosion cracking test in 25 °C, 0.1 M Na<sub>2</sub>S<sub>4</sub>O<sub>6</sub> solution (Reverse U-Bended Alloy 600 SE+, Noise peaks were measured for 80 hours in 1 Hz). Similarly in Fig. 2, background current noise band having a range of 10<sup>-9</sup>~10<sup>-10</sup> A/cm<sup>2</sup> was obtained. 15 cracking-related noise bands that are higher than those of the background noise band were detected and the first noise peak started at 990 seconds after testing. As shown in Fig. 4(b), the background potential noise band under 1\*10<sup>-5</sup> V were obtained but almost positive potential noise peaks were detected. Therefore, it is obvious that the electrochemical current noise is more effective than electrochemical potential noise to detect SCC.

Fig. 5 shows surface and cross section morphology after SCC test (reverse U-bending specimen) for 80 hrs of Alloy

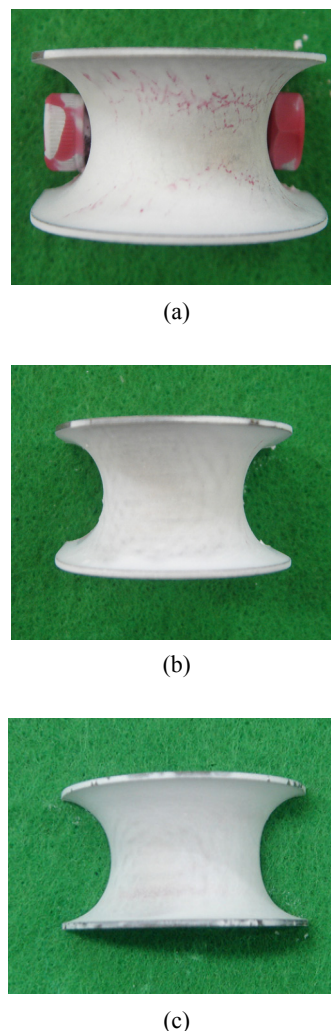


**Fig. 7.** Liquid penetration test for crack observation after SCC test in 25 °C, 0.1 M Na<sub>2</sub>S<sub>4</sub>O<sub>6</sub>, (a) 132 hrs, (b) 80 hrs, (c) 18 hr.



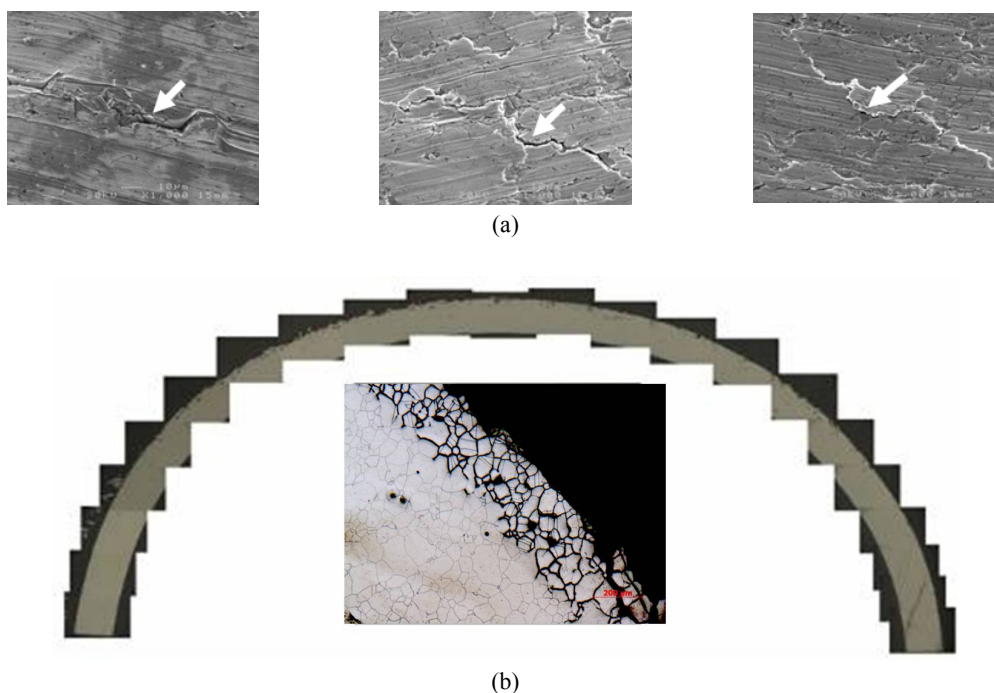
600 SE+ in 25 °C 0.1 M Na<sub>2</sub>S<sub>4</sub>O<sub>6</sub> solution. Similarly in Fig. 3, cracking mode was confirmed as intergranular cracking and most of cracks were generated near apex ± 20°.

Fig. 6 shows (a) current noise peaks and (b) potential noise peaks measured during stress corrosion cracking test in 25 °C, 0.1 M Na<sub>2</sub>S<sub>4</sub>O<sub>6</sub> solution (Reverse U-Bended Alloy 600 SE+). Noise was measured for 18 hours in 1 Hz). Like shown as Fig. 2 and Fig. 4, a background current noise band having a range of 10<sup>-9</sup>~10<sup>-10</sup> A/cm<sup>2</sup> was obtained. 3 cracking-related noise peaks that were higher than noise band were detected and first noise started at 555 seconds after testing. As shown in Fig. 6(b), a background potential noise band under 1\*10<sup>-5</sup> V was obtained but almost positive potential noise peaks were detected. Therefore, it is judged to be that electrochemical current noise is more effective than electrochemical potential noise to detect SCC.

Fig. 7 shows the liquid penetration test for crack observation after SCC test in 25 °C, 0.1 M Na<sub>2</sub>S<sub>4</sub>O<sub>6</sub>. (a) is the photo on the apex after 132 hrs testing, (b) is the photo on the apex after 80 hrs testing, and (c) is the photo on the apex after 18 hrs testing. As shown in Fig. 7(a), red colored cracks can be observed near the apex, but red colored cracks hardly observed by liquid penetration test in the case of short period testing such as 80 and 18 hours.

However, many cracks were observed by microscopic methods as shown in Fig. 8 for 18 hrs tested specimen. Fig. 8 shows surface and cross section morphologies after SCC test (reverse U-bending specimen) for 18 hrs of Alloy 600 SE+ in 25 °C 0.1 M Na<sub>2</sub>S<sub>4</sub>O<sub>6</sub> solution. Similarly in Fig. 3 and Fig. 5, cracking mode was confirmed as intergranular cracking and most of cracks were generated near apex ± 40°.

As discussed above, it is obvious that if cracks generate, its generation can be detected by electrochemical current noise method. However, current noises made by cracking had different values and moreover background noise bands having a broad band also generated during the test. Therefore, cracking-related noise criteria is needed to detect the cracking by SCC using electrochemical noise method. Fig. 9 shows noise criteria for determination of crack initiation time by (a) electrochemical noise monitoring during SCC test and evidences by (b) surface morphology and (c) cross section of crack after SCC test(reverse U-bending specimen) of sensitized Alloy 600(SE+) in 25 °C 0.1 M Na<sub>2</sub>S<sub>4</sub>O<sub>6</sub> solution. In this work, cracking-related noise was defined as the noise showing 5~10 times greater than the average value of background noise band on the base of 10 experiments. Therefore, crack initiation noise means the first noise greater than noise criteria among cracking-related noises and also it is considered that crack ini-



**Fig. 8.** Surface and cross section morphology after SCC test (reverse U-bending specimen) for 18 hrs of sensitized Alloy 600(SE+) in 25 °C 0.1 M Na<sub>2</sub>S<sub>4</sub>O<sub>6</sub> solution.

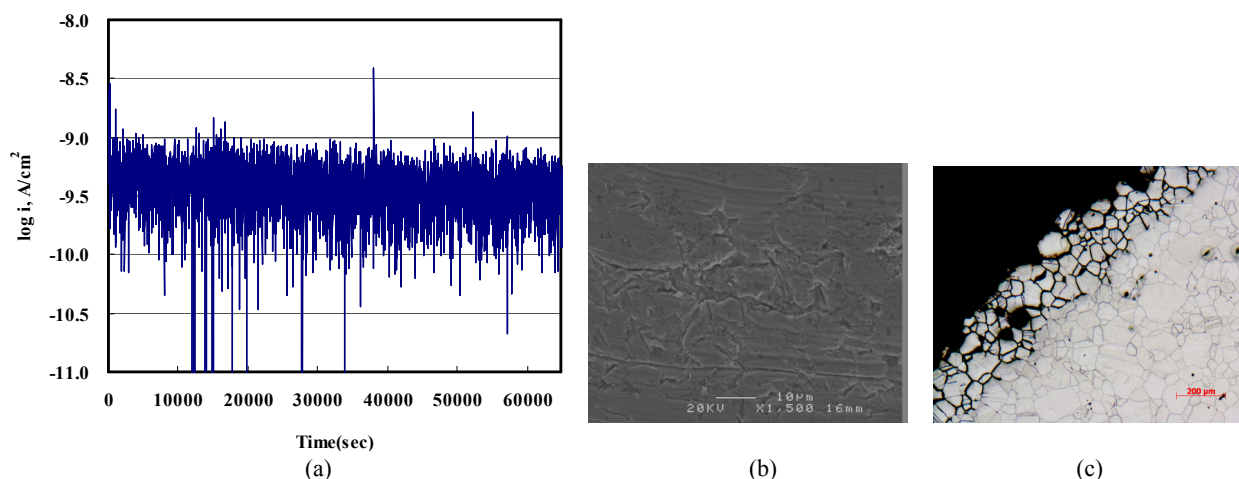


Fig. 9. Noise criteria for determination of crack initiation time by (a) electrochemical noise monitoring during SCC test and evidences by (b) surface morphology and (c) cross section of crack after SCC test(reverse U-bending specimen) of sensitized Alloy 600(SE+) in 25 °C 0.1 M  $Na_2S_4O_6$  solution.

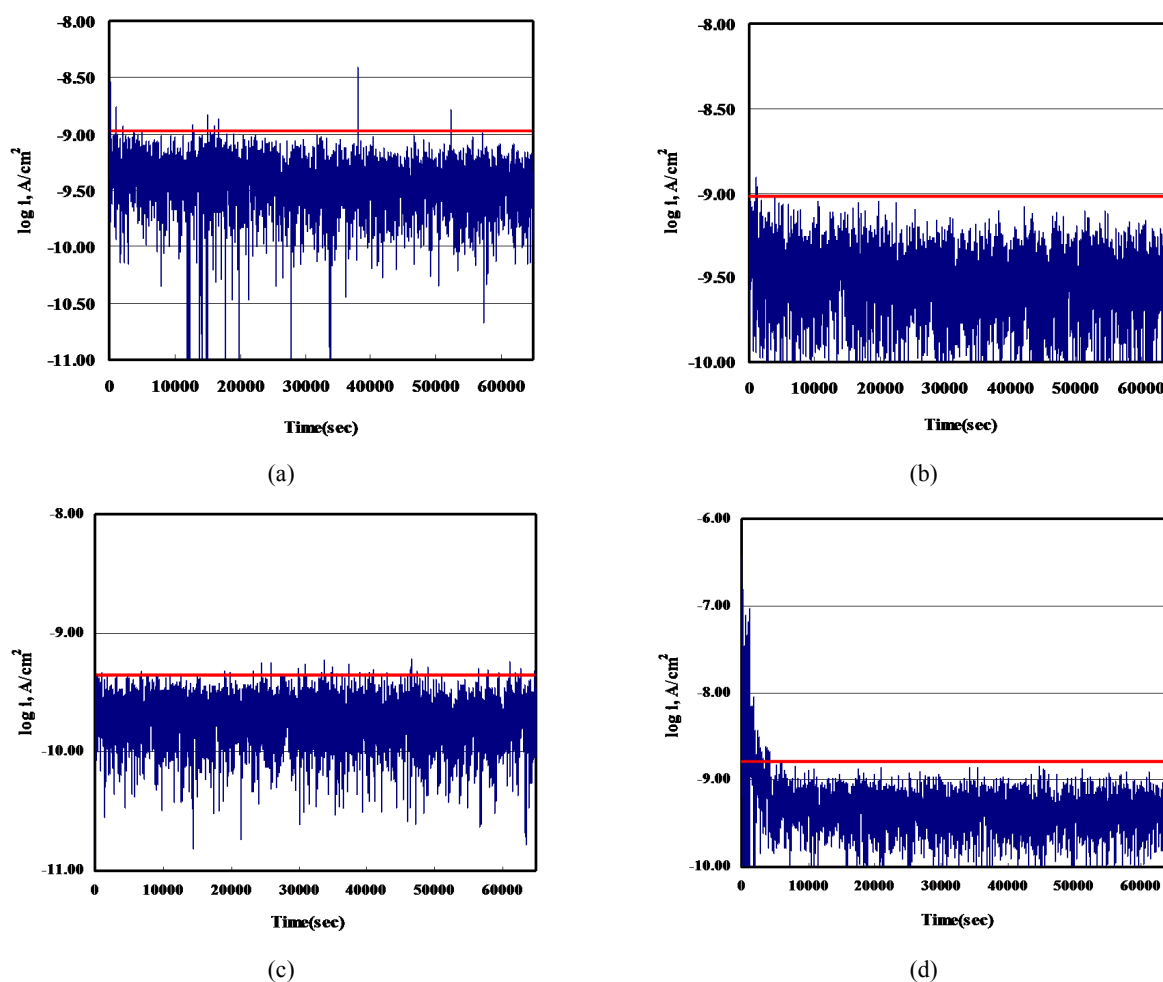
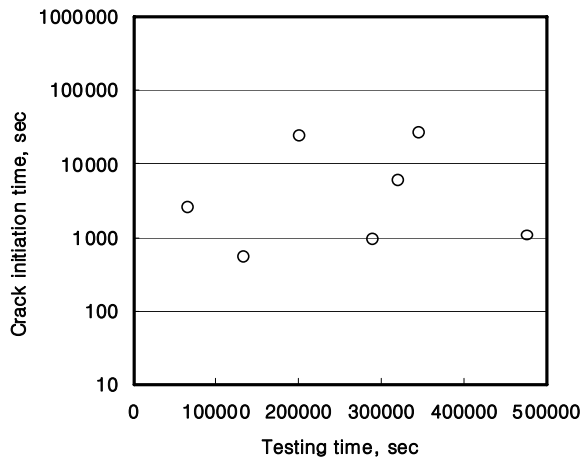


Fig 10. Cracking related noises greater than crack criteria in different SCC tests of sensitized Alloy 600(SE+) in 25 °C 0.1 M  $Na_2S_4O_6$  solution.



**Fig. 11.** Crack initiation time determined in different 7 SCC tests of sensitized Alloy 600(SE+) in 25 °C 0.1 M Na<sub>2</sub>S<sub>4</sub>O<sub>6</sub> solution.

tiation time is the time when the first noise signal is detected during the test.

Fig. 10 shows cracking related noises greater than crack criteria in different SCC tests of sensitized Alloy 600(SE+) in 25 °C 0.1 M Na<sub>2</sub>S<sub>4</sub>O<sub>6</sub> solution. Horizontal red lines in the Figs. means the crack criterion at each test. Fig. 11 shows crack initiation time determined in different 7 SCC tests of sensitized Alloy 600(SE+) in 25 °C 0.1 M Na<sub>2</sub>S<sub>4</sub>O<sub>6</sub> solution. In the case of 18 hours-tested specimen, crack initiates at 555 seconds after SCC test begins. In the case of 95 hours-tested specimen, crack initiates at 27,500 seconds after SCC test starts. As like these, many tests reveal very different initiation time and scattered data, and thus further researches should be needed to apply this technique to detect the SCC. However, average crack initiation time in this paper was determined as 9,046 seconds.

Crack length was determined using optical micrographs obtained in SCC test in 25 °C, 0.1 M Na<sub>2</sub>S<sub>4</sub>O<sub>6</sub>. Crack length in this work was defined as a straight distance from the surface to maximum crack tip. Fig. 12 shows crack propagation rates determined in different 7 SCC tests for sensitized Alloy 600SE+ in 25 °C 0.1 M Na<sub>2</sub>S<sub>4</sub>O<sub>6</sub> solution; (a) is apparent crack propagation rate and (b) is net crack propagation rate. Apparent crack propagation rate means the crack length divided by total test period but it didn't consider the effect of crack initiation process. However, net crack propagation rate is the crack length divided by  $\Delta T$ (= total test period - crack initiation time). As shown in Fig. 12, apparent and net crack propagation rates increased with SCC test time and average net crack propagation rate is  $1.18 \times 10^{-9}$  m/s.

As shown above, when test period was increased, crack propagation rate also was increased. This is contrary to

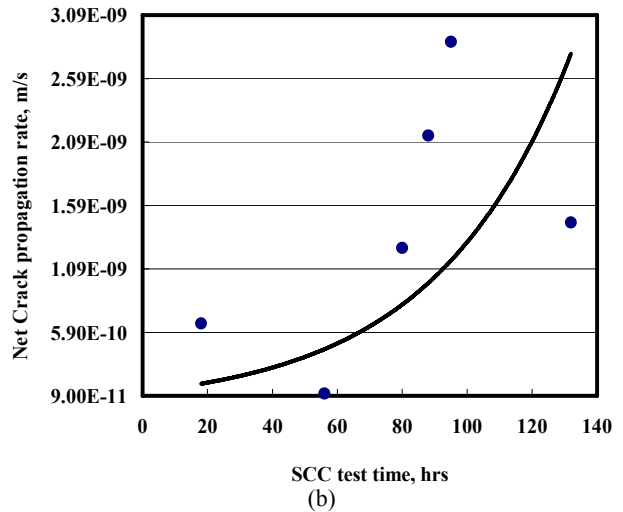
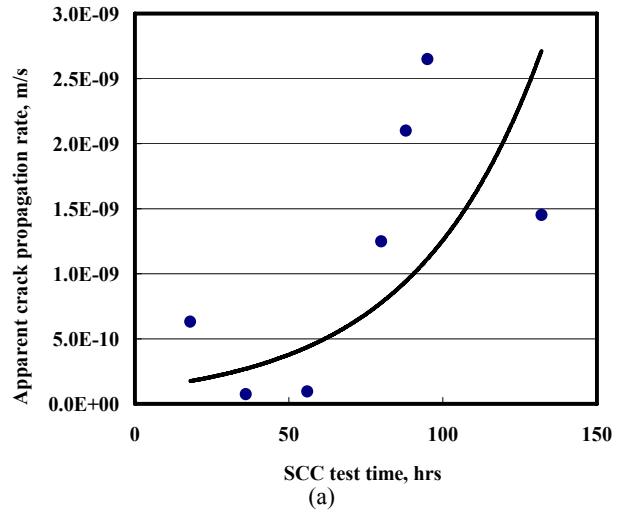
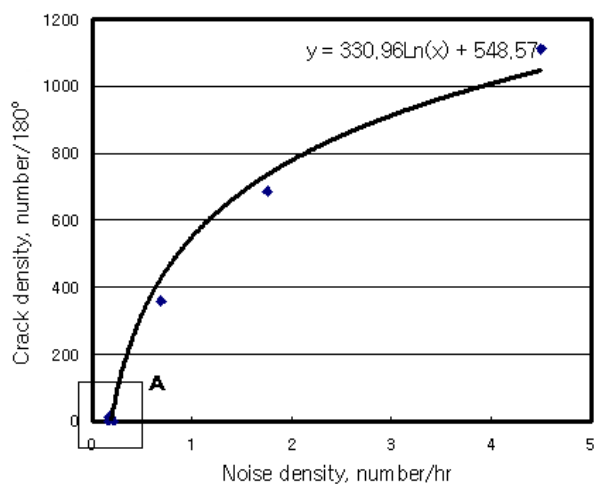


**Fig. 12.** Crack propagation rate obtained in different 7 SCC tests of sensitized Alloy 600 in 25 °C 0.1 M Na<sub>2</sub>S<sub>4</sub>O<sub>6</sub> solution; (a) apparent crack propagation rate, (b) net crack propagation rate.

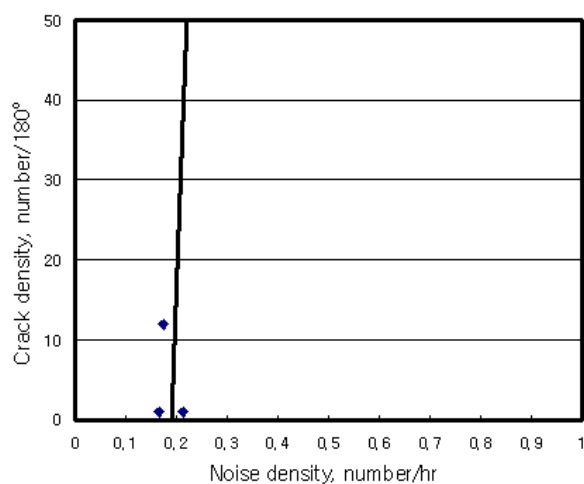
general trends. It is judge to be that this behavior was due to corrosion properties of sensitized Alloy 600 in the test solution. When a crack in reverse U-bended alloy (*i.e.* constant strain) initiates, crack propagation rate will be usually decreased because of stress release. However, the sensitized Alloy 600 corroded by intergranular mode in this test environment, and the crack propagation rate was increased because intergranular corrosion rate would be higher than the effect by stress release.

Fig. 13 shows the relationship between noise density and crack density obtained in different 7 SCC tests of sensitized Alloy 600 in 25 °C 0.1 M Na<sub>2</sub>S<sub>4</sub>O<sub>6</sub> solution ; (a) is noise density versus crack density and (b) is the expansion for Part A. Noise density can be defined noise numbers divided by test period, and crack density implies crack numbers divided by angle 180°. Regardless of test





(a)



(b)

**Fig. 13.** Relationship between noise density and crack density obtained in different 7 SCC tests of sensitized Alloy 600 in 25 °C 0.1 M Na<sub>2</sub>S<sub>4</sub>O<sub>6</sub> solution ; (a) Noise density versus Crack density, (b) Part A.

periods, crack density also increased as noise density increases. That is, it means that noise density was closely related to crack density, and its relationship showed the equation as like "crack density = 331 ln (noise density) + 549".

#### 4. Conclusions

1) When electrochemical noise monitoring technique is used to detect the cracking during SCC test, it was obvious that if cracks generate, its generation can be detected by electrochemical current noise. Cracking-related noise was defined as the noise showing 5~10 times greater than the

average value of background noise band. On the base of cracking-related noise, crack initiation time could be determined.

2) From SCC test (Reverse U-Bended type) and electrochemical noise monitoring in 25 °C, 0.1 M Na<sub>2</sub>S<sub>4</sub>O<sub>6</sub> solution (sensitized Alloy 600), average crack initiation time was determined as 9,046 seconds and, from its initiation time, it can be defined that net crack propagation rate is the crack length divided by ΔT (total test period - crack initiation time). Therefore, average net crack propagation rate was obtained to be 1.18x10<sup>-9</sup> m/s.

#### Acknowledgment

This work is funded by Korea Ministry of Education, Science and Technology.

#### References

1. S. S. Hwang, *Corros. and Protect.*, **6**, 65 (2007).
2. J. H. Kim, C. B. Bahn, and L. S. Hwang, *Corros. Sci. Tech.*, **3**, 198 (2004).
3. S. S. Hwang, J. S. Kim, K. E. Kasza, and J. Park, *Corros. Sci. Tech.*, **3**, 233 (2004).
4. S. S. Hwang, D. J. Kim, Y. S. Lim, J. S. Kim, J. Park, and H. P. Kim, *Corros. Sci. Tech.*, **7**, 187 (2008).
5. S. S. Hwang, M. K. Jung, J. Park, and H. P. Kim, *Corros. Sci. Tech.*, **8**, 188 (2009).
6. H. S. Chung and I. H. Kuk, *J. Corros. Sci. Soc. of Kor.*, **25**, 391 (1996).
7. D. H. Hur, J. Kim, D. H. Lee, Y. S. Kim, and J. S. Kim, *J. Corros. Sci. Soc. of Kor.*, **29**, 108 (2000).
8. Y. R. Yoo, h. Y. Chang, Y. S. Park, Y. B. Park, T. J. Chung, and Y. S. Kim, *Mater. Sci. Forum*, **475**, 4227 (2005).
9. H. P. Kim, C. Y. Oh, S. S. Hwang, I. H. Kuk, and J. S. Kim, *J. Corros. Sci. Soc. of Kor.*, **27**, 491 (1998).
10. H. Y. Ha, Master's thesis, Korea Advanced Institute of Science and Technology, Daejeon, Korea (2003).
11. J. R. Kearns, J. R. Scully, P. R. Roberge, D. L. Reichert, and J. L. Dawson, Eds., American Society for Testing and Materials, ASTM STP 1227, ASTM (1996).
12. J. J. Kim, *Corros. Sci. Tech.*, **3**, 14 (2004).
13. D. S. Seo, Master's thesis, Ulsan University, Ulsan, Korea (2005).
14. D. A. Eden, J. L. Dawson and D. G. John : UK Patent App.861158, US Patent 5139627, (1986).
15. Y. J. Tan, S. Bailey, and B. Kinsella, *Corros. Sci.*, **40**, 513 (1998).
16. F. Mansfeld, L. T. Han, C. C. Lee, C. Chen, G. Zhang, and H. Xiao, *Corros. Sci.*, **39**, 255 (1997).
17. C. C. Lee and F. Mansfeld, *Corros. Sci.*, **40**, 959 (1998).
18. F. Mansfeld, C. C. Lee, and G. Zhang, *Electrochim. Acta*, **43**, 435 (1998).
19. F. Mansfeld, Z. Sun, and C. H. Hsu, *Electrochim. Acta*,

- 46, 3651 (2001).
20. F. Mansfeld, Z. Sun, and C. H. Hsu, *Corros. Sci.*, **43**, 341 (2001).
21. M. Leban, V. Dolecek, and A. Legat, *Corros. Sci.*, **56**, 921 (2000).
22. E. H. Lee, K. M. Kim, and U. C. Kim, *Mater. Sci. Eng.*, **A449**, 330 (2007).
23. W. T. Tsai, M. J. Sheu, and J. T. Lee, *Corros. Sci.*, **38**, 33 (1996).
24. M. C. Tsai, W. T. Tsai, and J. T. Lee, *Corros. Sci.*, **34**, 741 (1993).
25. S. S. Hsu, S. C. Tsai, J. J. Kai, and C. H. Tsai, *J. Nucl. Mater.*, **184**, 97 (1991).